Journal of Nuclear Materials 381 (2008) 199–203

Contents lists available at ScienceDirect

Journal of Nuclear Materials

journal homepage: www.elsevier.com/locate/jnucmat

Microcracks in nuclear graphite and highly oriented pyrolytic graphite (HOPG)

Keyun Wen *, James Marrow, Barry Marsden

Materials Performance Centre, The University of Manchester, Grosvenor Street, Manchester M1 7HS, UK

ARTICLE INFO

PACS:
28.52.Fa

ABSTRACT

Microcracks with varied length and width are observed in nuclear grade graphite and highly oriented pyrolytic graphite (HOPG) by transmission electron microscopy. *In situ* observations show that these cracks tend to close up on heating the sample. The crystal dimensional change from *in situ* electron-irradiation also causes the closure of the cracks. Although some of the cracks may be identifiable as accommodation porosity (i.e. Mrozowski cracks), others appear to have already formed prior to carbonization and graphitization.

1. Introduction

Dimensional instability under irradiation is one of the main problems for the application of graphite in nuclear technology. Intensive efforts have been made to measure the irradiation induced dimensional changes of graphite and to understand the mechanism of these changes [1–3]. Because naturally occurring single crystals of graphite are too small for use in the measurements of irradiation induced dimensional change, highly oriented pyrolytic graphite (HOPG) has been used as an approximant of single crystal graphite [1,4]. Significant elongation along the c direction and slight contraction in the directions parallel to the basal plane were observed. The bulk volume changes in polycrystalline graphite during irradiation, on other hand, are less than those in a single crystal at low crystal strains because the *c-axis* crystal growth is absorbed by accommodation porosity. Once the crystal strain closes the porosity, the bulk volume change approaches that of the single crystal (HOPG) and eventually equals it [2].

The existence of porosity in crystallites of polycrystalline graphite was proposed by Mrozowski [5]. The porosity is in form of microcracks which have been referred to as Mrozowski cracks [6]. There have been earlier experimental studies on Mrozowski cracks [6,7]. In British reactor Grade A graphite, Sutton and Howard [7] observed, by electron microscopy of replicas, that cracks exist in parallel arrays, with individual crack lengths up to ~10 μm, mean width ~25 nm, and mean periodicity ~2 cracks/μm. In a more recent transmission electron microscopy (TEM) study of nuclear graphite, Hacker et al. [6] observed lenticular cracks, in broad agreement with the work of Sutton and Howard. However, their work shows that Mrozowski cracks exist in a large size distribution with some being less than 5 nm in width. Sutton and Howard [7] cited Harvey et al.'s earlier work that microcracks were observed in pyrolytically deposited graphite. Because of the importance of Mrozowski cracks in the understanding of the bulk volume changes of polycrystalline graphite during irradiation, this paper presents TEM observations of microcracks in nuclear graphite as well as in HOPG. The behaviour of the cracks in response to heating and *in situ* electron-irradiation is reported.

2. Experimental

The graphite samples used in this work include Pile Grade A (PGA) graphite, Gilsocarbon graphite, a SPI-1 grade (HOPG), and a baked carbon. Specimens for TEM were prepared by ion beam thinning with a Gatan PIPS using 4–4.5 keV Ar ions. Some specimens were prepared using microtome sectioning (i.e. cutting with a diamond knife to obtain samples of tens of nanometres thick or even thinner) for comparison to ensure that artefacts were not introduced during ion beam thinning. To prepare foils from bulk polycrystalline graphite, slices with a thickness of ~1 mm were cut from bulk samples. The slices were then ground and polished. The final thickness of the slices (foils) was about 20 μm. The foils were then cut into pieces of ~Φ3 mm by hand using a knife for ion beam thinning without further dimpling. TEM observations were carried out in a Philips CM 200 microscope and in a Tecnai F30 microscope operated at 200 KV and 300 KV, respectively. *In situ* heating experiments were carried out in the Philips CM 200 using a Gatan hot stage, at a heating rate of 10 °C/min to 800 °C. *In situ* irradiation was conducted at room temperature in the Tecnai F30 microscope operated at 300 KV. The electron flux and dose were not determined and are therefore unknown.

3. Results and discussion

Fig. 1(a) is a TEM image of PGA graphite. It is assumed to be a filler particle in which cracks of different length and width can

* Corresponding author.
E-mail address: k.wen@manchester.ac.uk (K. Wen).

0022-3115/$ - see front matter © 2008 Elsevier B.V. All rights reserved.
doi:10.1016/j.jnucmat.2008.07.012

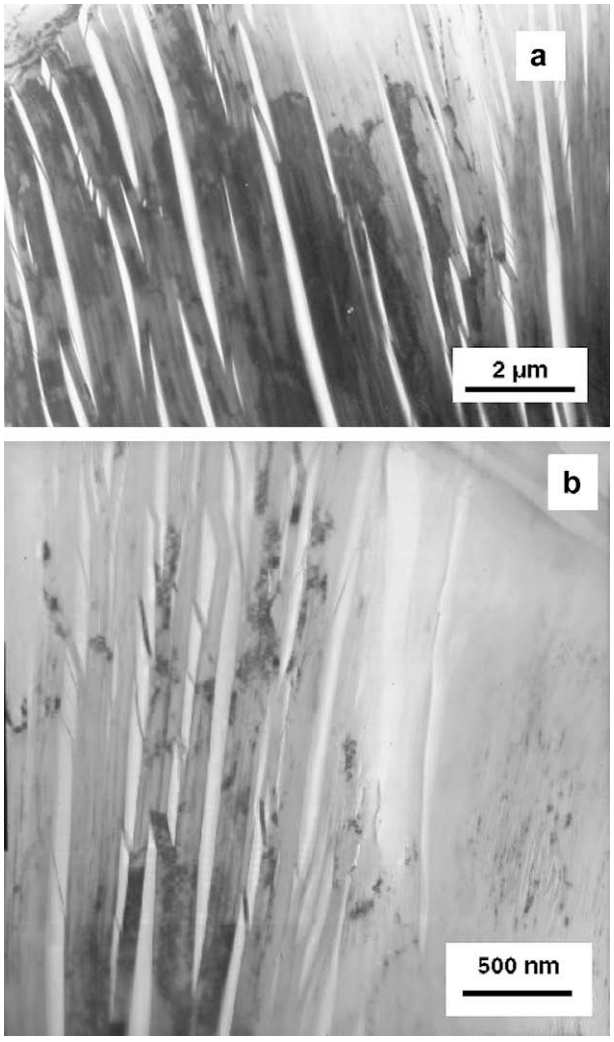

Fig. 1. (a) TEM image of microcracks in filler; (b) a filler/binder interface area with the cracking in binder (right) being much smaller than those in filler (left).

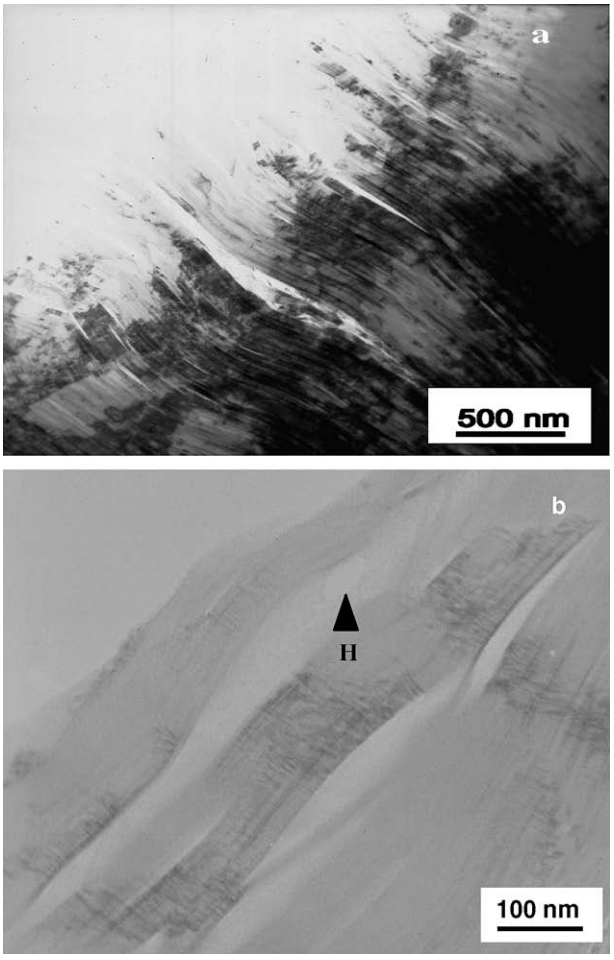

Fig. 2. (a) TEM image of filler in Gilsocarbon showing microcracks and bending of basal plane; (b) a hole, as indicated as H, is observed in a crack in Gilsocarbon. There is some material filled in the cracks.

be observed, with some cracks being longer than 10 μm. The cracks can be seen to have a lenticular (lens like) shape and to be bridged by crystallites. The width of the cracks can be as large as 100 nm. All the cracks were formed by cracking parallel to basal plane. Cracks with width of up to 200 nm were observed in PGA graphite in this study. In the right part of Fig. 1(b), a much finer structure can be observed. Both the thickness of the lamellae and the width of the cracks can be as small as about 10 nm. Fig. 1(b) may be from an interface between filler and binder, with the left part being the structure of a filler particle and the right part being the structure of binder.

TEM images of Gilsocarbon graphite are shown in Fig. 2. In Fig. 2(a), the cracks seem to be quite sparse. It is also noted that the basal planes bend in a wave form. Cracks with average length and width smaller than those in Fig. 1(b) can be observed in Fig. 2(b). A hole (indicated as H) can be seen in a crack in Fig. 2(b). The area in the crack is therefore not really empty, but seems to be filled with some material. The material exhibits a very low but homogeneous contrast which shows no change when the sample is tilted at large angles. High resolution TEM revealed no structural features in this material. The material is suggested to be a low density amorphous carbon. This is a general observation for almost all cracks observed. The cracks in Fig. 1 are also filled with such a low density material. Only the cracks which were very near the fringe of perforated holes were observed to be empty. This may be due to the faster removal of the low density amorphous carbon by the ion beam, compared to graphite.

To find whether the material in the cracks was a real feature or it was introduced during ion beam thinning. TEM observations were made on a sample of PGA prepared by microtome sectioning. The upper right part of Fig. 3 is a lamella which is too thick to be transparent to electrons. Some material can be seen to be attached to the lamella, as indicated by the arrows. This material exhibits low contrast and is considered to be the same as the low density carbon in the cracks in Figs. 1 and 2. It is therefore not an artefact of ion milling.

Fig. 4 shows a cross-section TEM image of a SPI-1 grade HOPG with the sample prepared by ion milling. Cracks with different length and width can be observed. The thickness of the lamellae which are separated by cracks varies from about half a micron to only tens of nanometres. Like in the microcracks in PGA and Gilsocarbon, there is also a low density carbon in the cracks of the SPI-1 grade HOPG and very fine lamellae with a thickness of ~2 nm were occasionally observed in the low density carbon. Similar cracks may be expected in HOPG fabricated by other manufacturers. Because those cracks in Fig. 4 are expected to close up during irradiation, the irradiation induced dimensional change along the *c*-axis of a perfect graphite crystal may be larger than that measured using HOPG.

A TEM image of baked carbon is shown in Fig. 5. Although no microcracks, such as those in Figs. 1 and 2, were observed in the

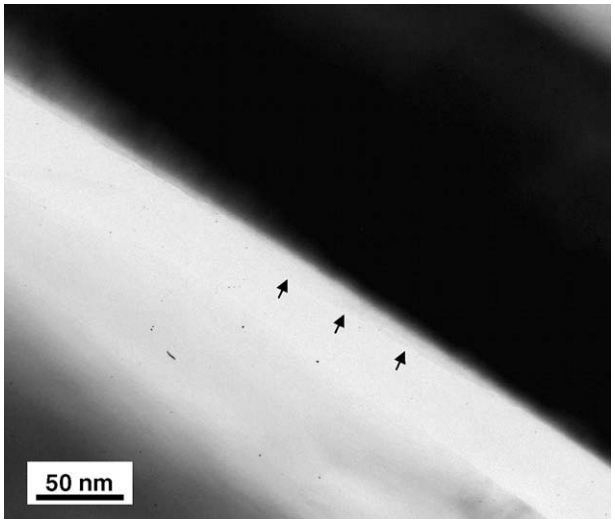

Fig. 3. TEM image of PGA graphite with sample prepared by microtome sectioning. Some material with low contrast as indicated by arrows can be observed to attach the side of a lamella.

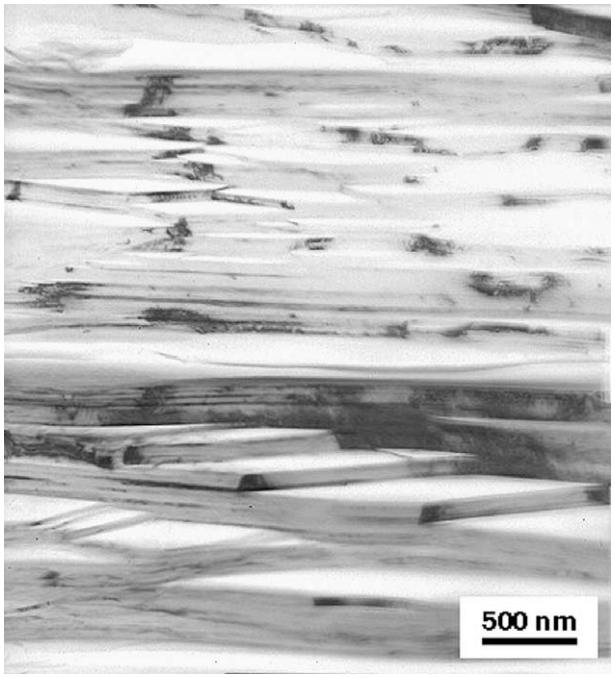

Fig. 4. Microcracks in a SPI-1 grade HOPG.

samples of backed carbon, some crack-like features, as indicated by arrows, can be observed in Fig. 5.

The results of the *in situ* heating experiment are shown in Fig. 6. Fig. 6(a) and (b) were taken from the same field at the same magnification but at different temperatures. Seemingly there is little change between the two images. When comparing carefully some features in the two images, for example, the triangle in the two images as enlarged in Fig. 6(c) and (d), changes induced by heating can be observed. The size of the triangle in Fig. 6(c) was reduced after the sample was heated to 800 °C (Fig. 6(d)) and the angle in the triangle as indicated contracted from 6.3° to 4.5° during heating. The cracks close up gradually, due to the thermal expansion along the *c-axis* of the surrounding crystallites. High resolution measurements of this displacement are in progress.

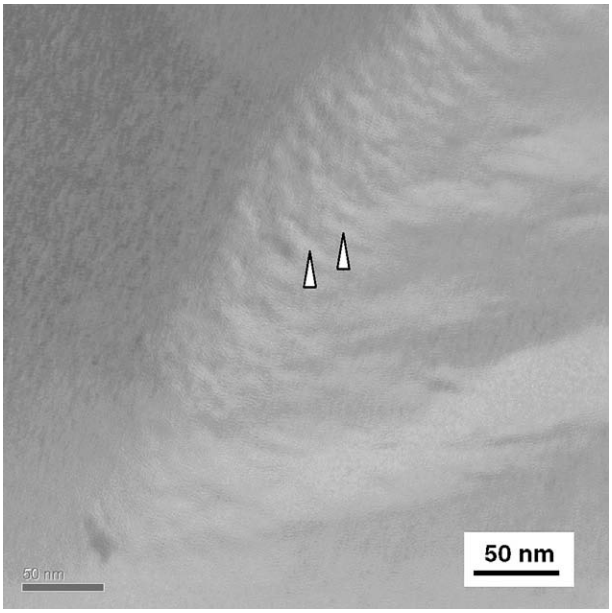

Fig. 5. TEM image of a baked carbon, some crack-like features as indicated can be observed.

Fig. 7 shows the results of the *in situ* electron-irradiation. There are two cracks in Fig. 7(a), one is about 60 nm in width and the other has a width of only ~10 nm. The electron beam was positioned to cover these two cracks. Because the TEM is equipped with a field emission gun, the density of the electron beam is very high, after only ~15 min, the larger crack was closed up (Fig. 7(b)). It is noted that after the closure of the larger crack, a feature with a contrast brighter than the surrounding region can be seen at around the centre line of the original crack. This feature may be formed from the low density carbon. At the lower right of Fig. 7(b), it is interesting to note that there is a small part of the crack, as indicated by the arrow, which is in the footprint of the electron beam and was therefore covered by the beam and should have closed up completely. It is only partly closed, with the two sides of the crack being not straight, but curved. This observation suggests that apart from irradiation induced dimensional change, other processes such as electron beam induced surface immigration of atoms may occur during irradiation. Fig. 7(c) is a high resolution TEM image showing the structure of the electron-irradiated graphite. Irradiation causes the breakage and bending of basal plane, and has been reported on neutron irradiated HOPG [3] and on electron-irradiated graphite [8,14]. The area between the two dashing lines in Fig. 7(c) corresponds to the feature with a brighter contrast in Fig. 7(b). It can be seen that the area has more disorder than its surroundings. The width of this area is about 6 nm, which is about tenth of the width of the original crack.

Lens-shaped cracks have also been reported in carbon/carbon composites fabricated by different techniques [9–11] and in carbon fibre [12]. There have been arguments over whether these cracks are real structure features, or are artefacts. Reznik et al. [10] proposed that the cracks were formed during mechanical thinning (dimpling). Fitz Gerald et al. [12] suggested that the cracks were most probably produced during ion beam thinning. Others suggested that the cracks may, in part, be a result of the grinding/polishing process and in part be a characteristic of microstructure of graphite [11,13]. The observation of the low density carbon in the samples prepared both by ion beam thinning and by microtome sectioning in this work suggests that microstructure features are retained during ion beam thinning and the microcracks are the

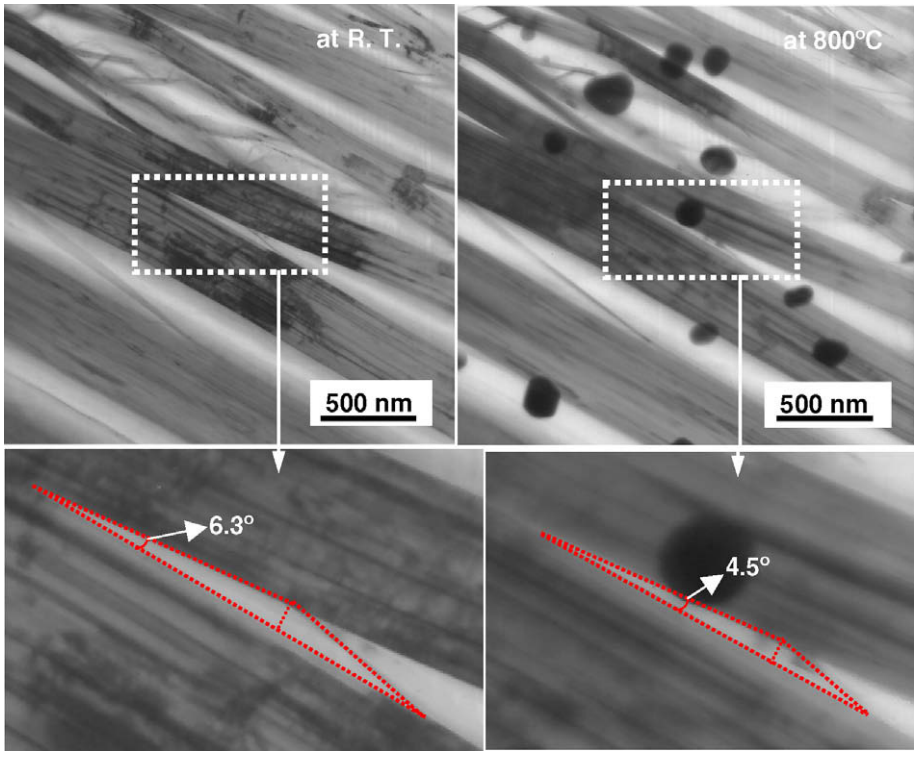

Fig. 6. Comparison of the images of a feature (triangle) at room temperature (a and c) and at 800 °C (b and d). Heating caused the contract of the triangle and the cracks show the trend to close upon heating.

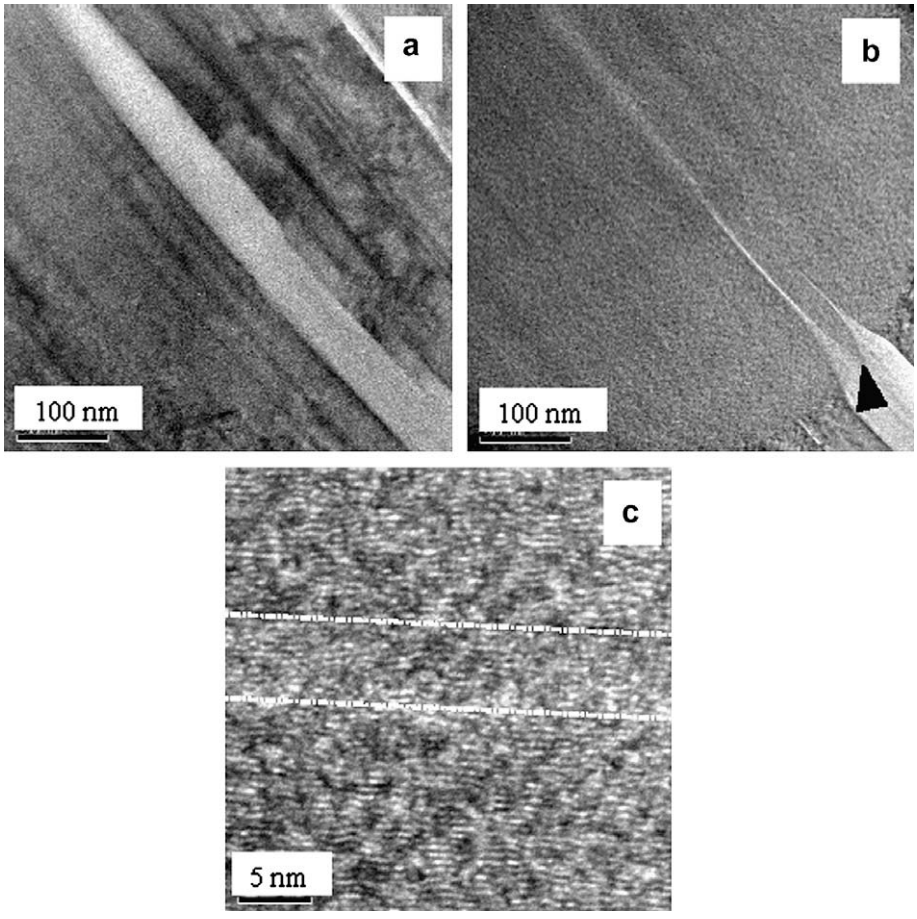

Fig. 7. *In situ* electron irradiation on graphite: (a) two cracks before irradiation; (b) closure of the cracks by electron irradiation. A feature with a contrast brighter than its surrounding can be observed. The arrow indicates a crack area which was covered by the electron beam but did not close up; (c) high resolution TEM image showing the structure of electron irradiated graphite; the area between the two dash lines corresponds to the features with a brighter contrast in (b).

characteristic features of nuclear graphite and most probably other synthetic graphites.

4. Conclusion

Transmission electron microscopy in this work provides some detailed information on the microcracks in nuclear graphite and HOPG. Both length and width of the cracks show a wide distribution, with lengths from tens of nanometres to more than 10 μm and width from several nanometres to about 200 nm. The cracks are not empty but are filled with low density carbon. The cracks tend to close upon heating and are closed up by electron-irradiation due to dimensional change of the graphite crystals.

Acknowledgements

We thank M. Faulkner for the help in preparing TEM samples by microtome sectioning. The authors gratefully acknowledge the support of the Nuclear Decommissioning Authority, Nexia Solutions for funding the research presented in this paper. This work was also carried out as part of the TSEC programme KNOO and as such we are grateful to the EPSRC for funding under grant EP/C549465/1. The views expressed in this paper are those of the authors and do not necessarily represent those of the sponsors.

References

[1] B.T. Kelly, W.H. Martin, P.T. Nettley, Philos. Trans. R. Soc. Lond. A 260 (1966) 37.
[2] B.T. Kelly, W.H. Martin, P.T. Nettley, Philos. Trans. R. Soc. Lond. A 260 (1966) 51.
[3] A. Asthana, Y. Matsui, M. Yasuda, K. Kimoto, T. Iwata, K. Ohshima, J. Appl. Cryst. 38 (2005) 361.
[4] R.J. Price, Carbon 12 (1974) 159.
[5] S. Mrozowski, Phys. Rev. 86 (1952) 622.
[6] P.J. Hacker, G.B. Neighbour, B. McEnaney, J. Phys. D: Appl. Phys. 33 (2000) 991.
[7] A.L. Sutton, V.C. Howard, J. Nucl. Mater. 7 (1962) 58.
[8] J. Koike, D.F. Pedraza, J. Mater. Res. 9 (1996) 1899.
[9] C.P. Ju, J. Don, P. Tlomak, J. Mater. Sci. 26 (1991) 6753.
[10] B. Reznik, D. Gerthsen, Carbon 41 (2003) 57.
[11] G.S. Rellick, P.M. Adams, Carbon 32 (1994) 127.
[12] J.D. Fitz Gerald, G.M. Pennock, G.H. Taylor, Carbon 29 (1991) 139.
[13] D.F. Pedraza, J. Koike, Carbon 32 (1994) 727.
[14] T. Tanabe, S. Muto, K. Niwase, Appl. Phys. Lett. 61 (1992) 638.